

Magnetization in pristine graphene with Zeeman splitting and variable spin-orbit coupling

F. Escudero[†], L. Sourrouille[†], J.S. Ardenghi^{†*} and P. Jasen[†]
[†]IFISUR, Departamento de Física (UNS-CONICET)
 Avenida Alem 1253, Bahía Blanca, Buenos Aires, Argentina

August 28, 2017

Abstract

The aim of this work is to describe the spin magnetization of graphene with Rashba spin-orbit coupling and Zeeman effect. It is shown that the magnetization depends critically on the spin-orbit coupling λ that is controlled with an external electric field. In turn, by manipulating the density of charge carriers, it is shown that spin up and down Landau levels mix introducing jumps in the spin magnetization. Two magnetic oscillations phases are described that can be tunable through the applied external fields. The maximum and minimum of the oscillations can be alternated by taking into account how the energy levels are filled when the Rashba-spin-orbit coupling is turned on. The results obtained are of importance to design superlattices with variable spin-orbit coupling with different configurations in which spin oscillations and spin filters can be developed.

1 Introduction

Graphene, a one-atom-thick allotrope, has become one of the most significant topics in solid state physics due to its two-dimensional structure as well as from its unique electronic properties ([1],[2],[3], [4], [5]). The carbon atoms form a honey-comb lattice made of two interpenetrating triangular sublattices, A and B that create specific electronic band structure at the Fermi level: electrons move with a constant velocity about $c/300$. In turn, the electronic properties are dictated by the π and π' bands that form conical valleys touching at the two independent high symmetry points at the corner of the Brillouin zone, the so called valley pseudospin [8]. In the absence of defects, electrons near these symmetry points behave as massless relativistic Dirac fermions with an effective Dirac-Weyl Hamiltonian [4] which allows to consider graphene as a solid-state toy for relativistic quantum mechanics. When the interaction between the orbital electron motion and spin degrees of freedom is taken into account, the spin-orbit coupling (SOC) induces a gap in the spectrum. SOC is the most important interaction affecting electronic spin transport in nonmagnetic materials. The use of graphene in spintronics ([9] and [10]) would require detailed knowledge of graphene's spin-orbit coupling effects, as well as discovering ways of increasing and controlling them. The SOC in graphene consists of intrinsic and extrinsic components ([11] and [12]). The intrinsic component of SOC is weak in the graphene sheet, although considerable magnitudes can be obtained in nanoscaled graphene ([13] and [14]). The extrinsic component, known as the Rashba spin-orbit coupling (RSOC) [15] can be larger than the intrinsic component [16]. The RSOC may be controlled by the application of external electric fields ([17] and [18]). On the other side, when a magnetic field is applied perpendicular to the graphene sheet, a discretization of the energy levels is obtained, the so called Landau levels [19]. These quantized energy levels still appear also for relativistic electrons, just their dependence on field and quantization

*email: jsardenghi@gmail.com, fax number: +54-291-4595142

parameter is different. In a conventional non-relativistic electron gas, Landau quantization produces equidistant energy levels, which is due to the parabolic dispersion law of free electrons. In graphene, the electrons have relativistic dispersion law, which strongly modifies the Landau quantization of the energy and the position of the levels. In particular, these levels are not equidistant as occurs in a conventional non-relativistic electron gas in a magnetic field. This large gap allows one to observe the quantum Hall effect in graphene, even at room temperature [20]. In turn, when magnetic fields are applied to solids an important effect called the de Haas-van Alphen (dHvA) [21] appears as oscillations of magnetization as a function of inverse magnetic field. This effect is a purely quantum mechanical phenomenon and is a powerful tool for mapping the Fermi surface, i.e. the electronic states at the Fermi energy ([22],[23]) and because it gives important information on the energy spectrum, it is one of the most important tasks in condensed matter physics. The different frequencies involved in the oscillations are related to the closed orbits that electrons perform on the Fermi surface. It has been predicted in graphene that magnetization oscillates periodically in a sawtooth pattern, in agreement with the old Peierls prediction [24], although the basic aspects of the behavior of the magnetic oscillations for quasi-2D materials remains yet unclear [25]. In contrast to 2D conventional semiconductors, where the oscillating center of the magnetization M remains exactly at zero, in graphene the oscillating center has a positive value because the diamagnetic contribution is half reduced with that in the conventional semiconductor [7]. From an experimental point of view, carbon-based materials are more promising because the available samples already allows one to observe the Shubnikov-de Haas effect ([26] and [27]) and then may be easier to interpret than quantum oscillations in its transport properties. Because the dHvA signal in 2D systems are free of the k_z smearing, it should be easier to obtain much rich information about the electron processes. In addition, the SOC, which is considerably large in graphene [28] plays an important role in the determination of the magnetic oscillations because of the fundamental difference with conventional semiconductor 2DEG.

Motivated by this phenonema, in the present paper we study the dHvA oscillations in the spin magnetization in graphene by taking into account the Rashba spin-orbit interaction modulated by a perpendicular external electric field and the Zeeman effect modulated by a constant magnetic field perpendicular to the graphene sheet. It is well known that each electron contributes with μ_B to the magnetization density if the spin is parallel to the applied magnetic field and $-\mu_B$ if it is antiparallel. Hence, if N_{\pm} is the number of electrons per area with spin parallel (+) or antiparallel (-), the magnetization density will be $M = \mu_B(N_+ - N_-)$. As it was said before, the introduction of a constant magnetic field introduces the Landau levels that are splitted by the Zeeman effect. The filling of these levels is not trivial in graphene due to its square root dependence in the Landau index. The degeneracy, that depends linearly on B , defines the number of states that are completely filled, but these levels may not be sorted in ascending order with intercalated spins. In fact, whenever the $n + 1$ Landau level with spin up is lower than the n Landau level with spin down, an enhancement of the spin magnetization will be obtained. This behavior can be alter drastically with the RSOC, because in this case, the ordering of the energy levels is not trivial. In this sense and since both the magnetic field and RSOC are externally controllable, in what follows the role of each of the parameters involved, as the electron density and the electric and magnetic field strength are discussed in relation to the maximum and minimum of the oscillations. The spin-orbit effects are important, besides the fundamental electronic and band structure and its topology, to understand spin relaxation, spin Hall effect and other effects such as weak (antilocalization). There are two main routes to implement spintronics devices: the giant magneto resistance effect (GMR) [29] and the spin effect field transistor (spin-FET) [30]. Both devices consists in a sandwich structure made of two ferromagnetic materials separated by a non-magnetic later in GMR and two dimensional electron gas in spin-FET. In this device, the spin-orbit coupling causes the electron spin to precess with a precession length determined by the strength of the spin-orbit coupling, which through a gate voltage becomes tunable. A detailed knowledge of the interplay of the the different parameters entering in the Hamiltonian is vital to fundamentally understand the spin-dependent phenomena in graphene.¹ This work will be organized

¹For a good review of spintronics in graphene see [31].

as follow: In section II, pristine graphene under a constant magnetic field with spin-orbit coupling and Zeeman splitting is introduced and the magnetic oscillations are discussed. In section III, N_+ and N_- populations as a function of B , the electron density and RSOC parameter is studied and the oscillations are computed and discussed. The principal findings of this paper are highlighted in the conclusion.

2 Magnetic oscillations with Zeeman splitting

For a self-contained lecture of this paper, a brief introduction of the quantum mechanics of graphene in a constant magnetic field in the long wavelength approximation will be introduced (see [5]). The Hamiltonian in one of the two inequivalent corners of the Brillouin zones can be put in a compact notation as (see [6] and [7])

$$H = v_F(\boldsymbol{\sigma} \cdot \boldsymbol{\pi}) + \frac{1}{2}\Delta_R(\boldsymbol{\sigma} \times \mathbf{s}) - \Delta_Z s_z \quad (1)$$

where $\boldsymbol{\sigma}$ are the Pauli matrices acting on the pseudospin space and \mathbf{s} are the Pauli matrices acting on the spin space. Δ_R is the extrinsic spin-orbit coupling that arise when an external electric field is applied perpendicular to the graphene sheet or from a gate voltage or charged impurities in the substrate ([32], [33] and [34]).² $\Delta_Z = \frac{q\mu_B}{2}B$ is the Zeeman energy that depends on the magnetic field strength. In the following we will write the extrinsic Rashba spin orbit coupling as $\Delta_R = \hbar\omega_y$. The quasiparticle momentum must be replaced by $\boldsymbol{\pi} = \mathbf{p} - e\mathbf{A}$, where e is the electron charge and \mathbf{A} is the vector potential which in the Landau gauge reads $\mathbf{A} = (-By, 0, 0)$. For the K valley, the third term can be written as $-i\Delta_R(\sigma_+ s_+ - \sigma_- s_-)$ where $\sigma_{\pm} = \sigma_x \pm i\sigma_y$ and $s_{\pm} = s_x \pm is_y$. This term describes a coupling between pseudospin and spin states, that is, a spin-flip process can be achieved by hopping an electron in the A sublattice with spin up to the B sublattice with spin down. The eigenvalues of the Hamiltonian of eq.(1) has been computed in [6] and [7] without the Zeeman term. By introducing this term the eigenvalues reads³

$$E_{n,s,l} = \frac{l\hbar}{\sqrt{2}} \sqrt{2\omega_Z^2 + 2n\omega_L^2 + \omega_y^2 - s\sqrt{16n\omega_Z^2\omega_L^2 + 4n\omega_L^2\omega_y^2 + \omega_y^4}} \quad (2)$$

where $l = +1(-1)$ is for the conduction (valence) band, $n = 0, 1, 2, \dots$ is the Landau level index and $s = \pm 1$ is the spin. The number of conduction electrons will be given by $N = n_e A$ where n_e is the electron density and A is the area of the graphene sheet. For simplicity, we can consider only conduction electrons, which implies that the added electrons are due to a gate voltage applied to the graphene sheet so that n_e can be varied as a function of V_G . When a magnetic field is applied, the energy is discretized and each level is degenerated with degeneracy $D = BA/\phi$, where ϕ is the magnetic unit flux. There is a critical magnetic field in which the degeneracy D equals the number of electrons N

$$B_C = n_e \phi \quad (3)$$

If we would consider only valence electrons, then $B_C \sim 80 \times 10^3 T$, which is an unfeasible experimentally. Nevertheless, B_C defined as in last equation will serve as an upper bound for the numerical calculations.

Let us consider the first case under study: graphene under a magnetic field with Zeeman effect. In this case, the energy levels can be found and reads

$$E_{n,s,l} = -s\hbar\omega_z + l\hbar\omega_L\sqrt{n} \quad (4)$$

²Intrinsic spin-orbit coupling Δ_{int} that contains contributions from the p orbitals and d orbitals (see eq.(10) of [11]) is neglected.

³In [35] it is discussed the intrinsic and extrinsic spin-orbit couplings and the quasi-classical limit for higher Landau levels.

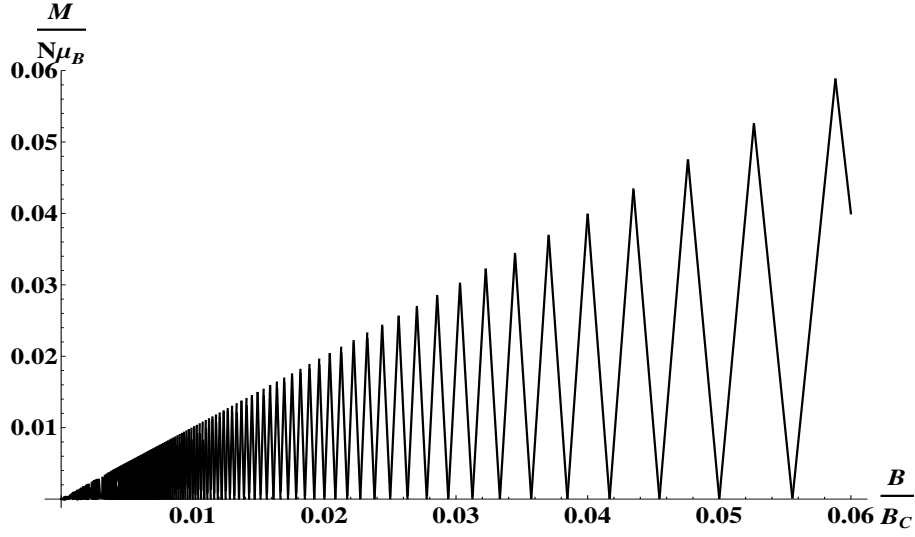


Figure 1: Dimensionless magnetization per number of electrons in the region where spin up and down levels do not mix.

being $s = \pm 1$ for spin up and down respectively, $n = 0, 1, 2, \dots$ is the Landau level index and $l = 1$ for the conduction band and $l = -1$ for the valence band. For the conduction band, electrons will start filling the lowest levels, so in the case in which $|\hbar\omega_z| < \frac{1}{2}|\hbar\omega_L|$, that is, when the Zeeman splitting is lower than half the separation between consecutive Landau levels, then the filling will be done considering the Landau index first and then the spin index.

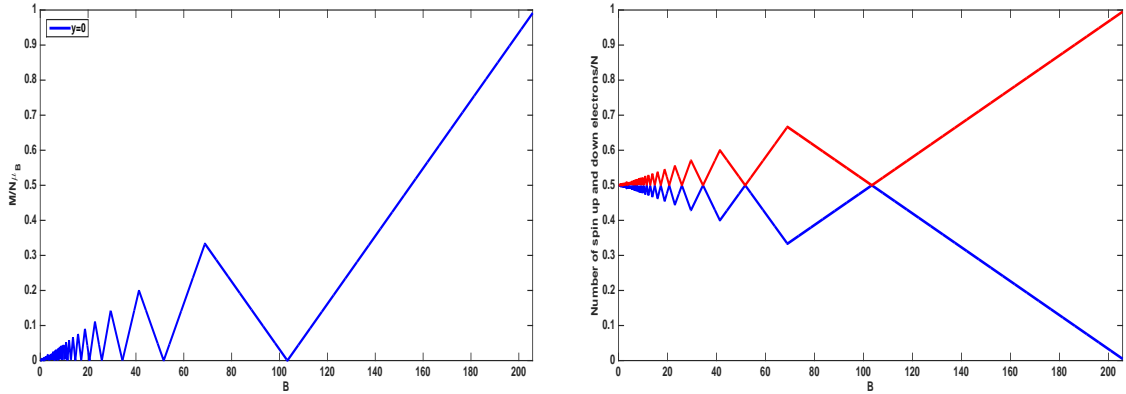


Figure 2: Left. Spin magnetization as a function of the magnetic field strength, where $n_e = 0.1\text{nm}^2$ and $A = 10\text{nm}^2$ without spin-orbit coupling. Right: Number of spin up and down electrons normalized with respect the number of electrons N .

This implies that if we consider the energy levels in ascending order, there will be no consecutive Landau levels with same spin filled. This assumption is fulfilled for normal systems, where ω_L is cyclotron frequency $\omega_L = \frac{eB}{m}$ and the Landau levels are $\hbar\omega_C(n + 1/2)$.

In this case, because ω_Z is proportional to B , then the condition $|\hbar\omega_z| < \frac{1}{2}|\hbar\omega_L|$ implies that $\frac{g\mu_B}{2} < \frac{\hbar e}{m}$. For graphene, due to the relativistic dispersion relation, ω_L is proportional to \sqrt{B} and the

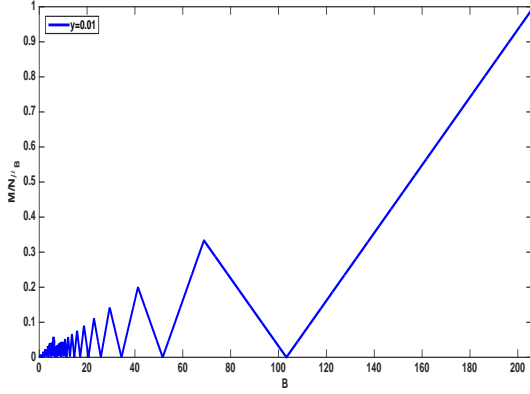


Figure 3: Spin magnetization for $y = 0.01\text{eV}$.

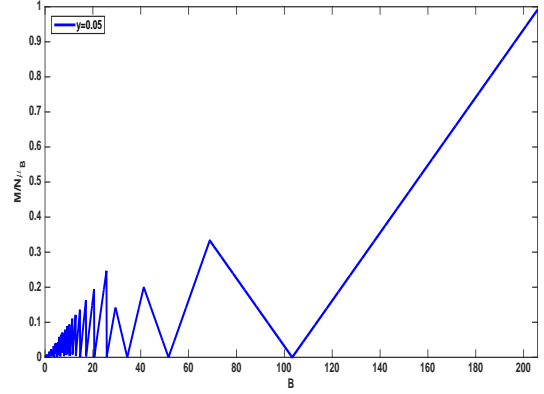


Figure 4: Spin magnetization for $y = 0.05\text{eV}$.

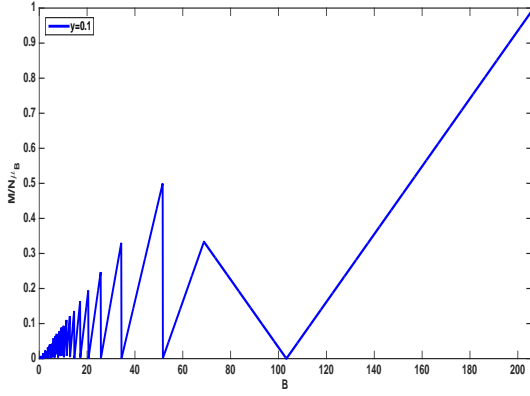


Figure 5: Spin magnetization for $y = 0.1\text{eV}$.

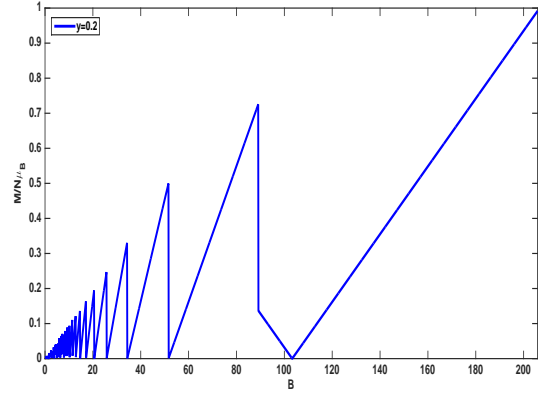


Figure 6: Spin magnetization for $y = 0.2\text{eV}$.

Landau levels increase as \sqrt{n} . Then if we write $\hbar\omega_z = \gamma_z B$ and $\hbar\omega_L = \gamma_L \sqrt{B}$, then the condition for no consecutive spin up or down filling is given by

$$B < \left(\frac{\gamma_L}{2\gamma_z} \right)^2 (\sqrt{n+1} - \sqrt{n})^2 \quad (5)$$

For graphene $\frac{\gamma_L}{2\gamma_z} \sim \frac{36.29}{2 \cdot 0.12} \sim 151.2$ (see [36] and [37]). Under this regime, the ordered energy levels can be written as

$$E_p = -(-1)^p \hbar\omega_z + \hbar\omega_c \sqrt{\frac{p}{2} - \frac{1}{4}(1 - (-1)^p)} \quad (6)$$

for p even we obtain the spin up levels and for p odd the spin down levels. The filling factor $\nu = B_C/B$ can be written as $\nu = q + \theta$, where $q = \lfloor \frac{B_C}{B} \rfloor$, where $\lfloor x \rfloor$ is the floor function defined as the largest integer less than or equal to x and $\theta = \nu - q$. The spin Pauli paramagnetism is given by the remaining term for the Landau filling which is proportional to λ

$$M = \mu_B(N_\uparrow - N_\downarrow) = N\mu_B \frac{B}{B_C} \left[\frac{1}{2} \left(1 - (-1)^{\lfloor \frac{B_C}{B} \rfloor} \right) + (-1)^{\lfloor \frac{B_C}{B} \rfloor} \left(\frac{B_C}{B} - \left\lfloor \frac{B_C}{B} \right\rfloor \right) \right]$$

where the difference $(N_\uparrow - N_\downarrow)$ is proportional to θ and the factor $(-1)^q$ selects the majority of spin up or down states in the last Landau level partially filled. In figure 1, the dimensionless magnetization per electron $M/N\mu_B$ is plotted against $x = \frac{B}{B_C}$.

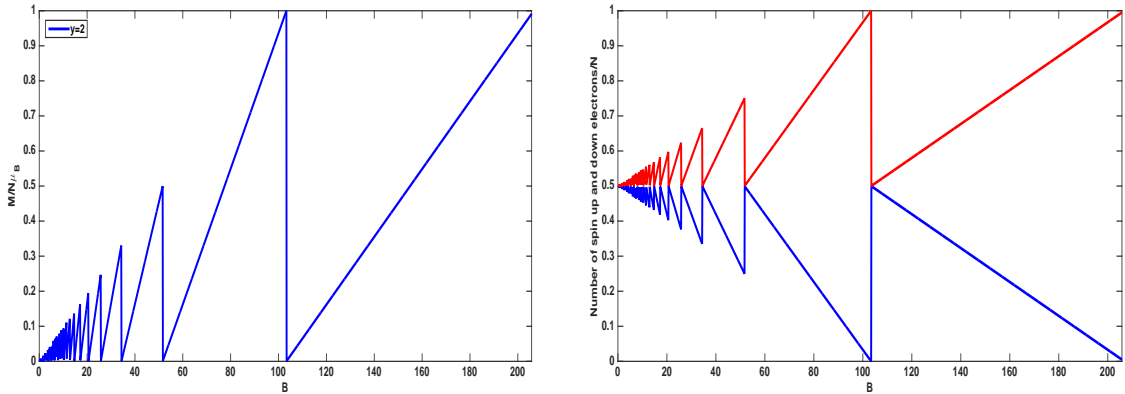


Figure 7: Left. Spin magnetization as a function of the magnetic field strength, where $n_e = 0.1\text{nm}^2$ and $A = 10\text{nm}^2$. The Rashba spin-orbit coupling is larger than the critical value where spin magnetization saturates. Right: Number of spin up and down electrons normalized with respect the number of electrons N .

It must be stressed that condition of eq.(5) depends on n and because $\sqrt{n+1} - \sqrt{n} < 1$ for $n > 1$, then for higher Landau levels the upper bound for B decreases and we must take into account the lowest Landau level completely filled $n = q = \lfloor \frac{B_C}{B} \rfloor$. This gives the condition for B

$$B < \left(\frac{\gamma_L}{2\gamma_Z} \right)^2 \left(\sqrt{\left\lfloor \frac{B_C}{B} \right\rfloor + 1} - \sqrt{\left\lfloor \frac{B_C}{B} \right\rfloor} \right)^2 \quad (7)$$

The jumps in the magnetization are well understood in terms of the filling of the Landau levels up to the Fermi level. Because the Fermi level indicates the lowest Landau level filled but the degeneration of each level is not a integer number, then when a level is completely filled, the Fermi level jumps and in consequence the magnetization. In the second regime, where $B \geq \left(\frac{\gamma_L}{2\gamma_Z} \right)^2 (\sqrt{n+1} - \sqrt{n})^2$, the energy levels will show consecutive Landau levels with the same spin filled. In this case, it is necessary to use numerical methods to sort the energy levels in ascending order taking into account if the level belongs to a spin up or down state. In figure 2, a sawtooth like behavior for the spin magnetization is obtained which is given by the spin up and down population, where we have used that $n_e = 0.1$. When $\nu = 2$, then $D = N/2$ which implies that the fundamental and first excited levels are completely filled. For this particular value of B , the first excited level are filled with spin down states. This behavior is shown in figure 2, where both population are identical for $B = B_C/2$. Between this value and $B = B_C$ ($\nu = 1$), the spin up population decreases linearly. The same behavior is expected for $\nu = l$ where $l = 1, 2, \dots$. For those values of B , the spin up and down population are identical. The spin magnetization peaks follows a linear behavior for high magnetic fields $M = \frac{B}{n_e \phi_0}$. For $B > n_e \phi_0$ the spin magnetization reaches a plateau given by $M = \mu_B N$.

2.1 Spin-orbit coupling

When an external electric field is applied perpendicular to the graphene sheet, the Bychkov-Rashba effect appears (see [11]). The parameter y that describes this interaction depends linearly with the external electric field strength. In figures 3, 4, 5 and 6, a sequence of plots for different values of y are

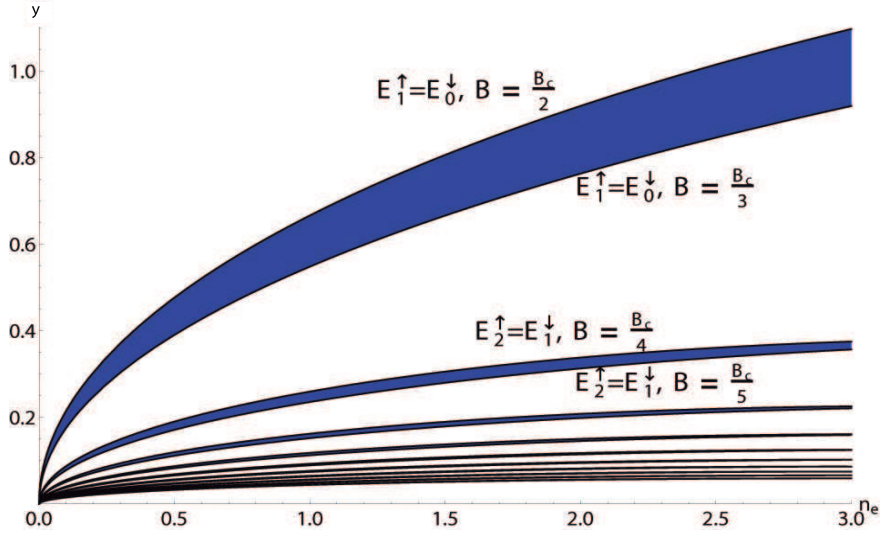


Figure 8: Rashba spin-orbit coupling y as a function of the electron density n_e . Blue regions between curves indicates those values of y where spin magnetization changes with respect the $y = 0$ case.

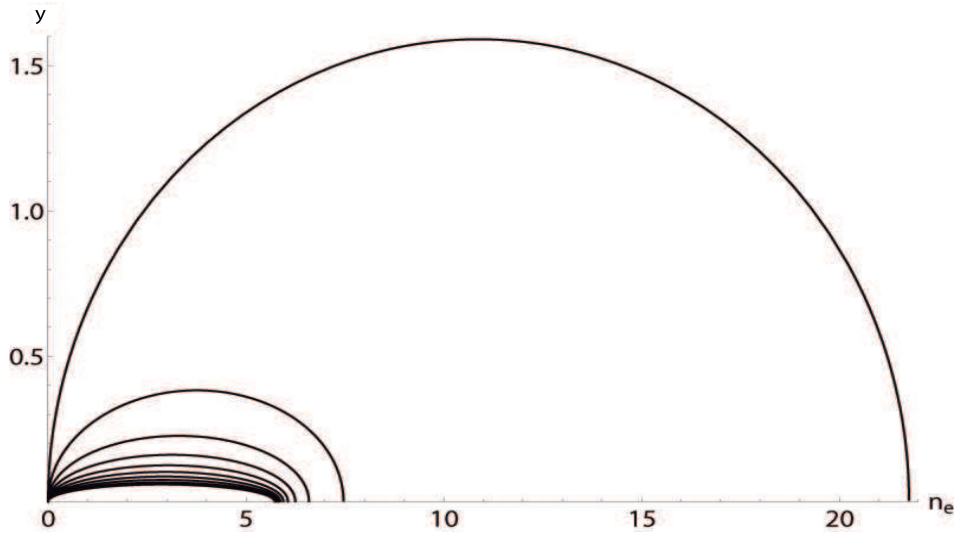


Figure 9: Rashba spin-orbit coupling y as a function of the electron density n_e . Each curve indicates the values of y where the spin magnetization jumps from 0 to $M = \mu_B N/2j$ where $j = 1, 2, 3, \dots$

shown, where $n_e = 0.1$ and $A = 10\text{nm}^{-2}$ ($N = 1$).⁴ As it can be seen in the supplementary material, there are set of values of y where there are no changes in the magnetization. These set of values are given when the spin up Landau energy level n is lower than the spin down energy level $n - 1$. For simplicity, let us consider that $\nu = 2$. Then only the two first Landau levels are completely filled when $y = 0$. In this case, because these two levels correspond to the spin up and down $n = 0$ Landau levels, then the spin magnetization vanishes because $N_+ = N_-$. When $y > 0$, there is a critical value $y_c^{(2)}$ where $E_{1,\uparrow} < E_{0,\downarrow}$ which implies that the two first Landau levels are spin up states. Then the magnetization jumps to a constant value $M = \mu_B N$. The condition $E_{1,\uparrow} < E_{0,\downarrow}$ implies that

$$\sqrt{2\gamma_Z^2 B^2 + 2y^2} \geq \sqrt{2\gamma_Z^2 B^2 + 2\gamma_L^2 B + y^2} - \sqrt{4\gamma_Z^2 B^2(4B\gamma_L^2 + y^2) + y^4} \quad (8)$$

and the solutions reads

$$y^2 \geq \frac{\gamma_L^2}{2} B - 2\gamma_Z^2 B^2 \quad (9)$$

which gives two solutions, one for positive values of y which is the case of interest. In turn, when $\nu = 3$, then $D = N/3$, then only the first three Landau levels are completely filled. For $y = 0$, there is no spin mixing and therefore the magnetization is positive and maximum. When $y > 0$ and in particular when $y > y_c^{(3)}$ then $E_{1,\uparrow} < E_{0,\downarrow}$, but in this case, when we increase the magnetic field strength, the degeneration increases, which implies that only the two first Landau levels are filled completely, which correspond to spin up states. Then, the magnetization increase as B does until we reach $B = \frac{B_C}{2}$. These considerations imply that there is a critical value $y_c^{(3)} < y < y_c^{(2)}$ defined from the equation $E_{1,\uparrow} = E_{0,\downarrow}$ when $B = \frac{n_e \phi_0}{2}$ for $y^{(2)}$ and when $B = \frac{n_e \phi_0}{3}$ for $y_c^{(3)}$ where the magnetization changes with respect the case $y = 0$. The regions for $y_c^{(j+1)} < y < y_c^{(j)}$ and n_e where the magnetization changes can be obtained from the condition $E_{j+1,\uparrow} = E_{j,\downarrow}$ when $B = \frac{n_e \phi_0}{j}$ for $y_c^{(j)}$ and $B = \frac{n_e \phi_0}{j+1}$ for $y_c^{(j+1)}$. In figure 8 these set of values are shown. For small values of y the regions tends to a continuum when $j \rightarrow \infty$. In turn, in figures 7, the spin magnetization as a function of B is shown when $y > y_c^{(1)}$, where the magnetization saturates. The set of magnetic fields $B_j = \frac{n_e \phi_0}{2j}$ are particularly important. For these values and

$$y_c^{(j)} = \sqrt{\frac{\frac{n_e \phi_0}{2j} (\gamma_L^2 - 4\gamma_Z^2 \frac{n_e \phi_0}{2j})^2 - 16(j-1)\gamma_Z^2 \gamma_L^2 (\frac{n_e \phi_0}{2j})^2}{4(j-1)\gamma_L^2 + 2\gamma_Z^2 - 8\gamma_Z^2 \frac{n_e \phi_0}{2j}}} \quad (10)$$

which is found by computing $E_{j+1,\uparrow} < E_{j,\downarrow}$ and replacing $B_j = \frac{n_e \phi_0}{2j}$, the magnetization jumps from $M = 0$ to $M_j = \mu_B N/2j$ (see figure 9). There are infinite mixes of Landau spin up and down states that are defined through the inequality $E_{n+r,\uparrow} \leq E_{r,\downarrow}$ which implies that

$$y^2 \geq \frac{16n\gamma_Z^2 \gamma_L^2 - (r\gamma_L^2 - 4\gamma_Z^2)^2}{8\gamma_Z^2 - 2(2n+r)\gamma_L^2} \quad (11)$$

These set of values are located between the regions described in figure 8.

These results are of importance to develop two-dimensional supertlattices structures by using graphene or silicene, which supports charge carriers behaving as massless Dirac fermions with graphene-like electronic band structure ([38] and [39]). Spin-orbit interaction in silicene can be 1000 times larger than of graphene, which implies that quantum spin Hall effect in silicene is experimentally accesible. Considering two semi-infinite graphene ribbons, that are employed as source and drain, and a drain voltage that introduces charge carriers with a concentration n_e it is possible to develop a superlattice of different graphene samples with specific values of y in series. By fixing the magnetic field strength in any of the critical values $B_j = \frac{n_e \phi_0}{2j}$, the possible values of y can be located over the curves in figure 9

⁴A supplementary video has been uploaded where the spin magnetization is plotted for increasing values of y for the particular case $n_e = 0.1\text{nm}^{-2}$.

in such a way to increase the spin polarized density of states across the superlattice. Different configurations can be obtained by developing superlattice with alternating constant electric fields in order to obtain spin flipping, which can be used as a spin down or up filter [40]. By applying Landauer-Büttiker formalism, the electronic behavior of Dirac fermions in the superlattice can be studied. The conductance will show resonant tunneling behavior depending on the number of barriers and barrier width [41]. In turn, the spin polarization lifetime can be controlled by the applied electric field that controls Rashba spin-orbit coupling [42] and [43]. It has been shown the angular range of the spin-inversion can be efficiently controlled by the number of barriers [44]. Magnons can be obtained in the superlattice structure by combining alternating applied electric fields, where the wavelength can be accommodated by the width of the middle graphene samples [45]. It is source of future works to develop graphene superlattice with different configurations of Rashba spin-orbit couplings and external magnetic fields.

Finally, to further explore the magnetic activation by changing the RSOC, we can consider the following setup: $N = 2$, that is, two conduction electrons only, $B = \frac{B_c}{2}$, where $D = 1$ which implies that we have to consider the first two Landau levels only. When $y = 0$, one electron occupies the ground state with spin up and the second electron the ground state with spin down which implies that the spin magnetization is zero. Suppose that we consider the action of a fast sudden perturbation in the system where the RSOC changes to $y = y_c^{(1)}$, where as we said before, $y_c^{(1)}$ is such that $E_{1,\uparrow} = E_{0,\downarrow}$ which is given in eq.(9). Then, because the first excited spin up level is below the ground state with spin down, the first two Landau levels filled are with spin up, which implies that M jumps to $M = 2\mu_B$. The transition amplitude is given by the inner product of both eigenstates. To obtain this value we can consider the anti-symmetric state for $y = 0$

$$|\psi_{M=0}\rangle = \frac{1}{\sqrt{2}} \left[|\varphi_{0,\uparrow}^{y=0}\rangle \otimes |\varphi_{0,\downarrow}^{y=0}\rangle - |\varphi_{0,\downarrow}^{y=0}\rangle \otimes |\varphi_{0,\uparrow}^{y=0}\rangle \right] \quad (12)$$

and the anti-symmetric state for $y = y_c^{(1)}$

$$|\psi_{M=2\mu_B}\rangle = \frac{1}{\sqrt{2}} \left[|\varphi_{0,\uparrow}^{y=y_c^{(1)}}\rangle \otimes |\varphi_{1,\uparrow}^{y=y_c^{(1)}}\rangle - |\varphi_{1,\uparrow}^{y=y_c^{(1)}}\rangle \otimes |\varphi_{0,\uparrow}^{y=y_c^{(1)}}\rangle \right] \quad (13)$$

where we can note that the state for the second electron is spin up. where we are considering that both electrons are not interacting. Each vector $|\varphi_{n,s}^{y=0}\rangle$ can be computed by considering the diagonalization of the Hamiltonian of eq.(1). This eigenfunctions are computed in [46] and [47] and we can write $|\varphi_{0,\uparrow}^{y=0}\rangle = \frac{1}{\sqrt{2L}} (\phi_0 \ \phi_0 \ 0 \ 0)$, $|\varphi_{0,\downarrow}^{y=0}\rangle = \frac{1}{\sqrt{2L}} (0 \ 0 \ \phi_0 \ \phi_0)$, $|\varphi_{0,\uparrow}^{y=y_c^{(1)}}\rangle = \frac{1}{\sqrt{2L}\sqrt{|\beta_1|^2+1}} (\beta_1\phi_0 \ 0 \ 0 \ \phi_0)$ and $|\varphi_{1,\uparrow}^{y=y_c^{(1)}}\rangle = \frac{1}{\sqrt{2L}\sqrt{|\alpha_1|^2+|\alpha_2|^2+|\alpha_3|^2+1}} (\alpha_1\phi_1 \ \alpha_2\phi_0 \ \alpha_3\phi_1 \ \phi_0)$, where $\phi_n(\xi) = \frac{\pi^{-1/4}}{\sqrt{2^n n!}} e^{-\frac{1}{2}\xi^2} H_n(\xi)$ where H_n are the Hermite polynomials of order n and $\xi = \xi = \frac{y}{l_B} - l_B k$, where $l_B = \sqrt{1/eB}$ is the magnetic length and k is the wavevector in the x direction. $2L$ is the total length of the graphene sample in the x direction. The coefficients β_1 , α_1 , α_2 and α_3 are obtained through the diagonalization of the Hamiltonian and reads

$$\beta_1 = \frac{i \left(\sqrt{2}\gamma_Z B + \sqrt{\gamma_L^2 B - 2\gamma_Z^2 B^2} \right)}{\sqrt{\gamma_L^2 B - 4\gamma_Z^2 B^2}} \quad (14)$$

$$\alpha_1 = \frac{i \left(\gamma_L^2 B + 2\sqrt{2}\gamma_Z B \sqrt{\gamma_L^2 B - 2\gamma_Z^2 B^2} \right)}{\sqrt{\gamma_L^2 B - 2\gamma_Z^2 B^2} \left(-\sqrt{2}\gamma_Z B + \sqrt{\gamma_L^2 B - 2\gamma_Z^2 B^2} \right)} \quad (15)$$

$$\alpha_2 = \frac{2i\sqrt{2}\gamma_L^2 B \sqrt{\gamma_L^2 B - 4\gamma_Z^2 B^2}}{2\gamma_L^2 B - 4\sqrt{2}\gamma_Z B \sqrt{\gamma_L^2 B - 2\gamma_Z^2 B^2}} \quad (16)$$

$$\alpha_3 = \frac{\gamma_L^2 B}{2 - \gamma_Z B + \sqrt{\gamma_L^2 B + 2\gamma_Z^2 B^2}} \quad (17)$$

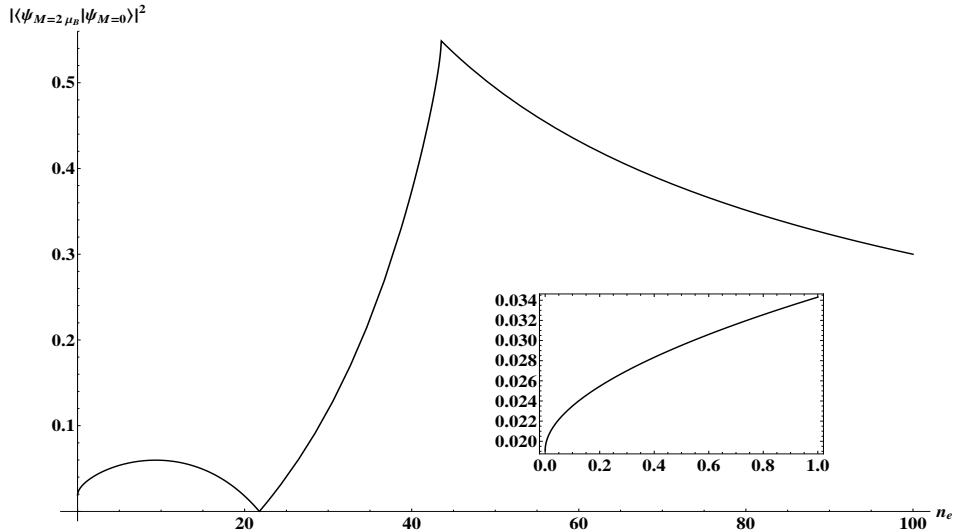


Figure 10: Transition amplitude for magnetic activation by a sudden perturbation $y = 0 \rightarrow y = y_c^{(1)}$ as a function of electron density n_e .

where we have to replace $B = \frac{B_c}{2}$ and $y = y_c^{(1)}$. In figure 10, the probability amplitude $|\langle \psi_{M=0} | \psi_{M=2\mu_B} \rangle|^2$ is plotted as a function of the electron density n_e . It is shown that the transition tends to zero as $n_e \rightarrow 0$ and a non-trivial zero for $n_e \sim 21\text{nm}^{-2}$. The curve in this region follows the behavior of the curve $y = y_c^{(1)}$ as it can be seen in figure 9, although it is not exactly a semicircle. For higher values of n_e , the probability amplitude tends to zero. Then it is possible to increase the spin magnetic transition for the specific value, where the probability amplitude is maximum for n_e . In this model we have not consider more than two electrons because in this case we should take into account the interactions between electrons in the same state, which can be done by considering the Laughlin wavefunctions [48] and the subtleties introduced by the fractional quantum Hall effect.

3 Conclusions

In this work we have examined the spin magnetization in pristine graphene with spin-orbit coupling and Zeeman splitting. The magnetization has been found as a function of the electron density, the magnetic field strength and the Rashba spin-orbit coupling parameter. We have derived and compared the maximum and minimum of the magnetization with and without spin-orbit coupling showing that for certain regions of the spin-orbit coupling parameter y and certain values of the electron density n_e , the magnetization jumps from zero to a constant value given $M_j = \mu_B N / 2j$ being N the number of electrons and $j = 1, 2, 3, \dots$ being an integer number that controls when a spin up state with Landau level $j + 1$ is lower than the spin down state with Landau level j . Moreover, these regions for y follows a complex relation with n_e that numerically shows certain values of y where magnetization is not altered by y . These results show that it is possible to obtain spin filters or spin oscillations by considering different superlattice configurations, where the inner graphene samples can alternate the applied electric field in such a way to fix the magnetic field strength in those values where the Landau spin up and down states mix. Finally, we have studied the probability amplitude for a sudden change of the Rashba spin-orbit coupling from the non-magnetic state $M = 0$ to $M = 2\mu_B$ when there are two electrons, $B = \frac{n_e \phi_0}{2}$ and $y = y_c^{(1)}$, showing that the transition has a peak for $n_e > 0$ and a non-trivial zero.

4 Acknowledgment

This paper was partially supported by grants of CONICET (Argentina National Research Council) and Universidad Nacional del Sur (UNS) and by ANPCyT through PICT 1770, and PIP-CONICET Nos. 114-200901-00272 and 114-200901-00068 research grants, as well as by SGCyT-UNS., J. S. A. and L. S. are members of CONICET., F. E. is a fellow researcher at this institution.

5 Author contributions

All authors contributed equally to all aspects of this work.

References

- [1] K. S. Novoselov, A. K. Geim, S. V. Morozov, D. Jiang, M. I. Katsnelson, I. V. Grigorieva, S. V. Dubonos and A. A. Firsov, *Nature*, **438**, 197 (2005).
- [2] A.K. Geim and K. S. Novoselov, *Nature Materials*, **6**, 183 (2007).
- [3] Y. B. Zhang, Y.W. Tan, H. L. Stormer and P. Kim, *Nature*, **438**, 201 (2005).
- [4] A. H. Castro Neto, F. Guinea, N. M. R. Peres, K. S. Novoselov and A. K. Geim, *Rev. Mod. Phys.*, **81**, 109 (2009).
- [5] M. O. Goerbig, *Rev. Mod. Phys.*, **83**, 4, (2011).
- [6] E. I. Rashba, *Phys. Rev. B* **79**, 161409, (2009).
- [7] F. Zhen-Guo, W. Zhi-Gang, L. Shu-Shen and Z. Ping, *Chin. Phys. B*, **20**, 5 058103 (2011).
- [8] J. McClure, *Phys. Rev.*, **104**, 666, (1956).
- [9] I. Zutic, J. Fabian, and S. D. Sarma, *Rev. Mod. Phys.* **76**, 323 (2004).
- [10] J. Fabian, A. Matos-Abiague, C. Ertler, P. Stano, and I. Zutic, *Acta Phys. Slov.* **57**, 565 (2007).
- [11] S. Konschuh, M. Gmitra, and J. Fabian, *Phys. Rev. B*, **82**, 245412 (2010).
- [12] J. Balakrishnan, G.K. Koon, M. Jaiswal, A.H.C. Neto, B. Ozyilmaz, *Nat. Phys.* **10** 1038 (2013).
- [13] C.L. Kane, E.J. Mele, *Phys. Rev. Lett.* **95** 226801 (2005).
- [14] C.L. Kane, E.J. Mele, *Phys. Rev. Lett.* **95** 146802 (2005).
- [15] Y.A. Bychkov, E.I. Rashba, *JETP Lett.* **39** 78 (1984).
- [16] R. Decker, Y. Wang, V.W. Brar, W. Regan, H.Z. Tsai, Q. Wu, W. Gannett, A. Zettl, M.F. Crommie, *Nano Lett.* **11** 2291 (2011).
- [17] C. Ertler, S. Konschuh, M. Gmitra, J. Fabian, *Phys. Rev. B*, **80** 041405 (2009).
- [18] D.A. Abanin, P.A. Lee, L.S. Levitov, *Phys. Rev. Lett.*, **96** 176803 (2006).
- [19] S. Kuru, J. Negro and L. M. Nieto, *J. Phys.: Condens. Matter*, **21**, 455305 (2009).
- [20] Y. Zheng and T. Ando, *Phys. Rev. B*, **65**, 245420 (2002).
- [21] W. de Haas and P. van Alphen, *Proceedings of the Academy of Science of Amsterdam*, **33**, 1106–1118 (1930).

- [22] I. Meinel, T. Hengstmann, D. Grundler, D. Heitmann, W. Wegscheider and M. Bichler , *Phys. Rev. Lett.*, **82**, 819 (1999).
- [23] M. P. Schwarz, M. A. Wilde, S. Groth, D. Grundler, C. Heyn and D. Heitmann, *Phys. Rev. B*, **65**, 245315 (2002).
- [24] S. G. Sharapov, V. P. Gusynin and H. Beck, *Phys. Rev. B*, **69**, 075104 (2004).
- [25] T. Champel and V.P. Mineev, *Philos. Mag. B*, **81**, 55 (2001).
- [26] S. Uji, J.S. Brooks, and Y. Iye, *Physica B*, **299** 246-247 (1998).
- [27] Z.M. Wang, Q.Y. Xu, G. Ni, and Y.W. Du, *Phys. Lett. A*, **314**, 328 (2003).
- [28] A. Varykhalov, J. Sanchez-Barriga, A. M. Shikin, C. Biswas, E. Vescovo, A. Rybkin, D. Marchenko, and O. Rader , *Phys. Rev. Lett.* **101** 157601 (2008).
- [29] P. Grünberg, R. Schreiber, Y. Pang, M. B. Brodsky and H. Sowers, *Phys. Rev. Lett.*, **57**(19):2442, (1986).
- [30] S. Datta and B. Das, *Appl. Phys. Lett.*, **56**:665, (1990).
- [31] N. Kheirabadi, A. Shafiekhani and M. Fathipour, *Superlattices and Microstructures*, **74**, 123-145 (2014).
- [32] G.Y. Wu, N.-Y. Lue, *Phys. Rev. B*, **86**, 045456 (2012) .
- [33] A. Manjavacas, S. Thongrattanasiri, D.E. Chang, F.J.G. deAbajo, *New J. Phys.*, **14**, 123020 (2012).
- [34] G. Burkard, *Nat. Nanotech.*, **7**, 617 (2012).
- [35] V. Yu. Tsaran and S. G. Sharapov, *Phys. Rev. B*, **90**, 205417 (2014).
- [36] S. Das Sarma, S. Adam, E. H. Hwang, and E. Rossi, *Rev. Mod. Phys.*, **83**, 407 (2011).
- [37] M.O. Goerbig, R. Moessner, B. Doucot, *Phys. Rev. B*, **74**, 161407 (2006).
- [38] C. C. Liu, W. Feng, and Y. Yao, *Phys. Rev. Lett.*, **107**, 076802 (2011).
- [39] S. Cahangirov, M. Topsakal, E. Akturk, H. Sahin, S. Ciradi, *Phys. Rev. Lett.*, **102**, 236804 (2009).
- [40] N. Pournaghavi M. Esmailzadeh, S. Ahmadi, M. Farokhnezhad, *Solid State Commun*, **226**, 33-58 (2016).
- [41] X-S. Wang, M. Shen, X-T. An and J. J. Liu, *Phys. Rev. Lett.*, **380**, 1663-1667 (2016).
- [42] X-T. An, *Phys. Lett. A*, **379**, 723-727 (2015).
- [43] D. Wang, G. Jin, *Phys. Lett. A*, **378**, 2557-2560, (2014).
- [44] F. Sattari, . Faizabadi, *Superlattices and microstructures*, **81**, 80-87 (2015).
- [45] Y. Hajati and Z. Rashidian, *Superlattices and microstructures*, **92**, 264-277 (2016).
- [46] J. S. Ardenghi, P. Bechthold, E. Gonzalez, P. Jasen and A. Juan, *Eur. Phys. J. B*, **88**: 47 (2015).
- [47] J. S. Ardenghi, P. Bechthold, E. Gonzalez, P. Jasen and A. Juan, *Physica B*, **433**, 28-36 (2014).
- [48] R. B. Laughlin, *Phys. Rev. Lett.*, **50**, 1395 (1983).